NANO LETTERS

Letter

pubs.acs.org/NanoLett

The Quantum Magnetism of Individual Manganese-12-Acetate Molecular Magnets Anchored at Surfaces

Steffen Kahle,[†] Zhitao Deng,[†] Nikola Malinowski,[†] Charlène Tonnoir,[†,∥] Alicia Forment-Aliaga,[†,⊥] Nicha Thontasen,[†] Gordon Rinke,[†] Duy Le,[‡] Volodymyr Turkowski,[‡] Talat S. Rahman,[‡] Stephan Rauschenbach,[†] Markus Ternes,*[,†] and Klaus Kern[†,§]

[†]Max Planck Institute for Solid State Research, Heisenbergstrasse 1, D-70569 Stuttgart, Germany

[‡]Department of Physics, University of Central Florida, Orlando, Florida 32816, United States

[§]Institut de Physique de la Matière Condensée, Ecole Polytechnique Fédérale de Lausanne, CH-1015 Lausanne, Switzerland

Supporting Information

ABSTRACT: The high intrinsic spin and long spin relaxation time of manganese-12-acetate (Mn_{12}) makes it an archetypical single molecular magnet. While these characteristics have been measured on bulk samples, questions remain whether the magnetic properties replicate themselves in surface supported isolated molecules, a prerequisite for any application. Here we demonstrate that electrospray ion beam deposition facilitates grafting of intact Mn_{12} molecules on metal as well as ultrathin insulating surfaces enabling submolecular resolution imaging by scanning tunneling microscopy. Using scanning tunneling spectroscopy we detect spin excitations from the magnetic ground state of the molecule at an ultrathin boron nitride decoupling layer. Our results are supported by density functional theory based calculations and establish that individual Mn_{12} molecules retain their intrinsic spin on a well chosen solid support.

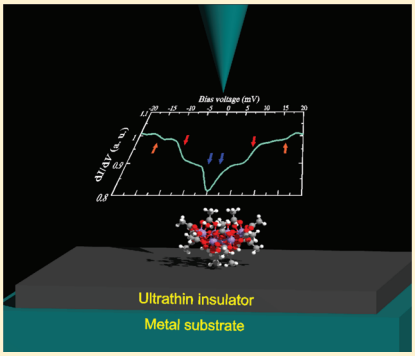

KEYWORDS: *Electrospray mass spectrometry, ion beam deposition, molecular magnetism, scanning tunneling microscopy, inelastic tunneling spectroscopy*

At the interface between classical and quantum mechanical description single molecular magnets (SMM)[1] offer novel approaches in information storage,[2] spintronics,[3] and quantum computation.[4] In SMMs, spin carrying atoms are arranged within a molecular framework such that their magnetic states can be described as a single giant spin. Mn_{12}, composed of a $Mn_{12}O_{12}$ core surrounded by 16 acetate groups (Figure 1a), represents a prototypical molecular magnet with a total spin $S = 10$. Resulting from its large magnetic anisotropy D, it has a magnetization reversal barrier height of $-DS^2 = 6$ meV in bulk, enough to produce very long spin relaxation times at low temperatures.[5] Throughout many studies, the immobilization of manganese-12-acetate (Mn_{12}) molecules at surfaces has been found to be difficult, as its fragile structure changes easily upon deposition, thus altering its magnetic properties.[6−10] In particular, the controlled in-vacuo deposition of Mn_{12} is hindered by its thermal instability.

Here we use electrospray ion beam deposition (ES-IBD) as gentle deposition method[11−13] to bring Mn_{12} molecules on atomically well-defined metal and ultrathin insulating surfaces and study their structure and magnetic properties by scanning tunneling microscopy (STM) and spectroscopy (STS). Figure 1b illustrates the schematic setup of the ES-IBD system. Time-of-flight (TOF) mass spectra for different declustering potentials ($V_{decl.}$), a parameter which adjusts the collision energy between the ion beam and the background gas (see Supporting Information) are shown in Figure 1c. While at low $V_{decl.}$ a peak corresponding to $Mn_{12}Ac_{17}^{1-}$ is found besides the intact Mn_{12} molecule, at high $V_{decl.}$ the loss of acetate groups is the main source of defected molecules. To further decrease contamination the Mn_{12} ion-beams were mass selected before deposition using a quadrupole ion guide (Figure 1d).

After room temperature deposition of Mn_{12} on Cu(001), Au(111), and a monolayer of BN on Rh(111), we measure STM topographies. On Cu(001), we observe randomly distributed molecules (Figure 2a) meaning that Mn_{12} is immobile at room temperature. In contrast, on Au(111) the molecules are mobile and can be imaged stably only after cooling down to 40 K. At low coverage, they preferably occupy the fcc part of the Au(111) surface reconstruction starting at elbow sites (Figure 2b). Only after those have been filled the molecules occupy the hcp part of the surface (see Supporting Information). In contrast to bare metal surfaces, the BN monolayer on Rh(111) is chemically very inert[14] and has shown to be an excellent electronic decoupling layer.[15] The deposition of Mn_{12} on the BN surface results in a random distribution of individual molecules in the depressions of the BN corrugation (Figure 2c).

On all surfaces, we identify individual molecules from their size of $(2.3 \pm 0.4) \times (1.9 \pm 0.4)$ nm^2 and a voltage dependent

Received: November 24, 2011
Published: December 19, 2011

   dx.doi.org/10.1021/nl204141z | *Nano Lett.* 2012, 12, 518−521

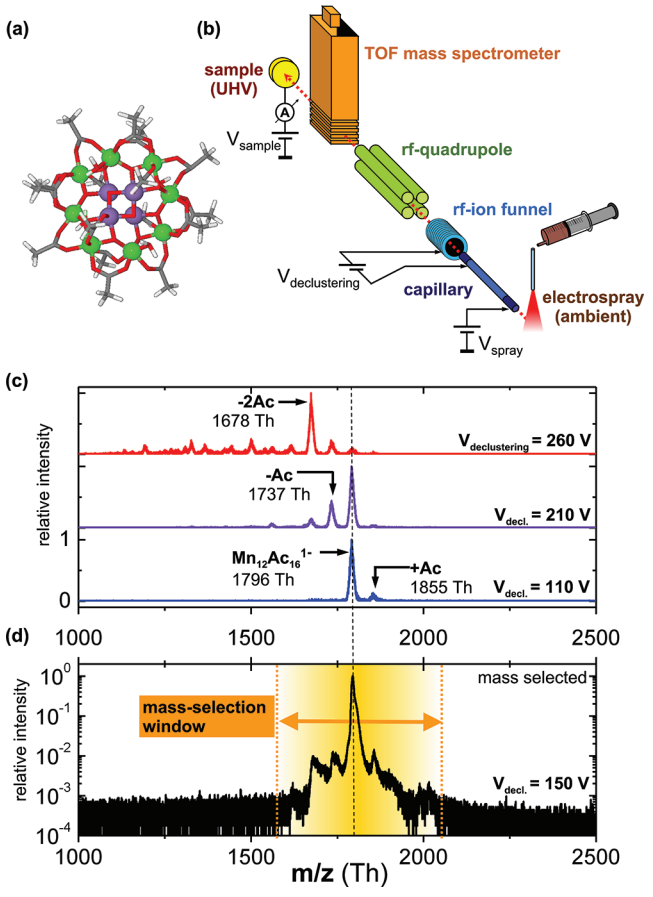

Figure 1. Electrospray ion beam deposition (ES-IBD) of Mn_{12} molecular magnets. (a) Structure of the $Mn_{12}O_{12}(CH_3COO)_{16}$ molecule (Mn_{12}). Balls represent manganese atoms of two different charge and spin state: green, Mn^{3+} (S = 2); violet, Mn^{4+} (S = 3/2). Red (gray, white) sticks represent bonds to oxygen (carbon, hydrogen). All Mn atoms of the same spin state are coupled ferromagnetically while Mn atoms of different spin are coupled antiferromagnetically resulting in a ground state of S = 10. (b) Simplified schematic of the ES-IBD. A solution of Mn_{12} molecules is electrosprayed at ambient conditions and mass selectively deposited onto the sample in ultra high vacuum (UHV) (10^{-10} mbar). (c) Mass spectra show the intact molecule (1796 Th) and fragments due to acetate loss (1737 Th, 1678 Th) for different declustering potentials. (d) Mass spectrum of a mass selected beam at V_{decl} = 150 V for deposition (log scale). The total contamination by fragmented molecules is suppressed to <5% intensity.

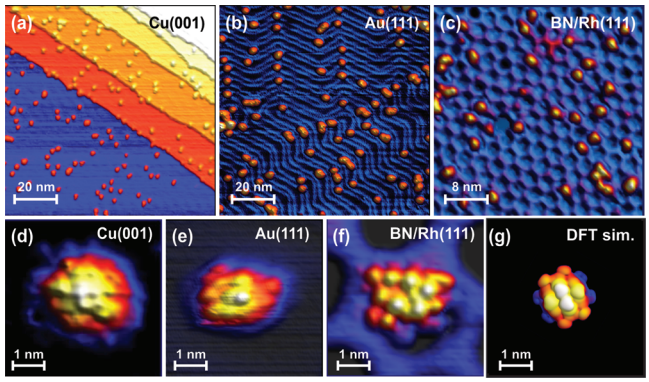

Figure 2. STM topographic images of Mn_{12} molecules deposited on different surfaces. (a) On Cu(001) immobile molecules are randomly distributed over the surface at 300 K. (b) On Au(111), molecules are found preferably at the elbow sites of the herringbone reconstruction (T = 40 K). (c) On the BN/Rh(111) surface, molecules adsorb in the depressions of the BN corrugation (T = 1.5 K). (d–f) Images of individual molecules reveal an intramolecular structure identified as the acetate groups. Different adsorption geometries can be observed. (g) Comparison with the DFT calculation of the free molecule. Tunneling parameters: (a) V = +2 V, I = 100 pA; (b) +2 V, 80 pA; (c) +0.9 V, 100 pA; (d) +2.5 V, 120 pA; (e) +2 V, 80 pA; (f) −1 V, 45 pA.

apparent height between 0.25 and 0.7 nm.[7] Detailed imaging of the molecules (Figure 2d–f) shows good agreement to an intact molecule, simulated by density functional theory (DFT) calculation (Figure 2g and Supporting Information). The characteristic submolecular structure with lobes of approximately 0.5 nm size corresponds to the acetate groups of the SMM as seen in DFT.

To address the question of whether these SMMs still exhibit their striking magnetic properties, we have applied inelastic spin-flip spectroscopy at low temperature T = 1.5 K (Figure 3). We measure the differential conductance dI/dV on top of the Mn_{12} molecules and observe symmetric features around the Fermi energy only when the molecule is adsorbed on the thin BN insulator. Spectra in zero and at applied magnetic field perpendicular to the surface show a step-like structure in dI/dV which corresponds to peaks in the numerically derivated d^2I/dV^2 as shown in Figure 3d. The innermost step is usually the most prominent one and can be found at 1–2 meV, while the outer steps can be observed in a range up to 16 meV. On bare metal surfaces we do not observe such dominant features presumably due to the quenching of the spin.

To interpret these features we omit for the moment the many spin nature of the system by using the giant spin approximation in which S = 10 is fixed. The magnetic anisotropy is responsible for the zero-field splitting of the spin eigenstates in the z-projection m and leads to a degenerate ground state for $|S,m\rangle$ = $|10, -10\rangle$ and $|10, 10\rangle$ (Figure 3b). Excitations of the SMM by the tunneling electrons are detected as increasing differential conductance when the energy of the tunneling electrons is large enough to excite this state and the spin-flip selection rules are obeyed (Figure 3c).[16,17] The model with fixed S reduces possible magnetic excitations to changes of m, explaining the inner step of the spectra as the excitation from $|S,m\rangle$ = $|10, \pm10\rangle$ to $|10, \pm9\rangle$.

To cover also excitations that change S, we go beyond the giant spin picture and calculate possible spin excitations using a Hamiltonian in which the spin of each individual Mn atom inside the Mn_{12} molecule interacts with its neighbors and the external magnetic field $\vec{B}$. We use an effective 8-spin model[18] where linear Heisenberg exchange, magnetic anisotropy of the individual Mn atoms, and Dzyaloshinsky–Moriya interactions are taken into account. The parameters in the Hamiltonian are derived from the DFT calculations (see Supporting Information), which were performed with the substrate approximated by one layer of BN. The Hamiltonian leads to a ground state of S = 10. Calculation of the spin-flip excitations that obey the selection rules shows three low-energy features at 0 T (10 T) of 1.2 (1.8), 5.5 (6.2), and 10.9 (11.6) meV as displayed in Figure 3e. Similar energies have been found previously also in neutron scattering experiments on bulk Mn_{12} samples[19,20] and in break-junction experiments.[21] Comparing the theoretical results with the experimental data reveals good agreement with the observation of three peaks but differences in the positions especially at the energetically higher peaks, which is not surprising due to the simplifications of the model in which different adsorption geometries are not taken into account.

dx.doi.org/10.1021/nl204141z | Nano Lett. 2012, 12, 518–521

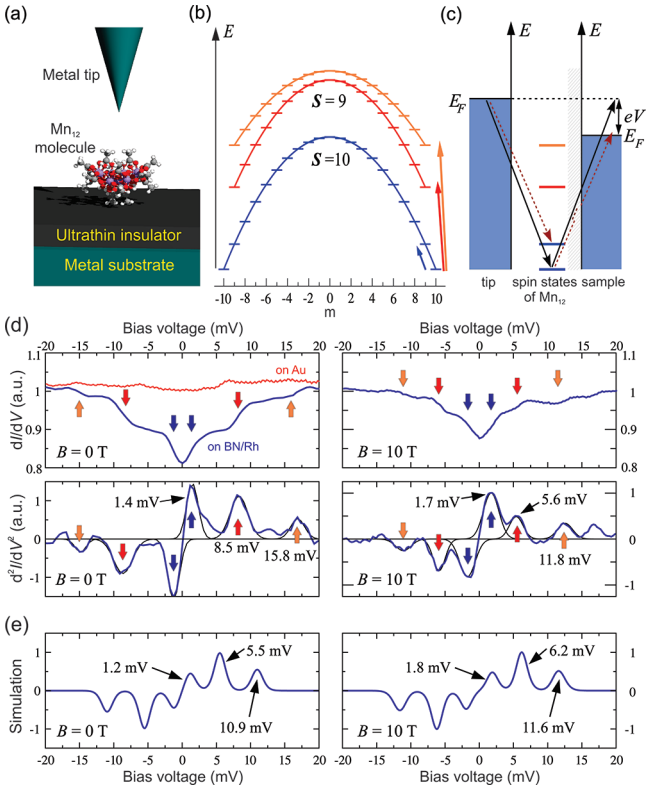

Figure 3. Tunnel spectroscopy on individual Mn_{12} molecules adsorbed on BN/Rh(111). (a) Schematic of the tunneling geometry. (b) Schematic energy diagram of a Mn_{12} molecule in the giant spin approximation $H = -DS_z^2$ with $S = 10$ ground state and easy axis anisotropy $D > 0$ without external magnetic fields applied. Arrows indicate possible excitations by interaction with the tunneling electron which obey the spin selection rules $\Delta S = 0, \pm 1$ and $\Delta m = 0, \pm 1$. (c) Cotunneling processes between the metal tip and the BN/Rh(111) sample via the Mn_{12} molecule. Full arrows, elastic tunneling; dashed red arrows, inelastic tunneling process which excites the internal spin system of the Mn_{12} . The latter process opens a new conduction channel $\sigma_{inelastic}$ when the bias voltage eV exceeds the energy difference between initial and final state and contributes to the total differential conductance $\sigma = \sigma_{elastic} + \sigma_{inelastic}$. (d) Typical dI/dV and d^2I/dV^2 spectra (V_{set} = 100 mV, I_{set} = 20 pA, T = 1.5 K) of a Mn_{12} molecule adsorbed on a BN/Rh(111) surface at $B = 0$ T (left) and $B =$ 10 T (right) reveal low energy spin-flip excitations which manifest themself as steps (peaks) in the dI/dV (d^2I/dV^2) spectrum (blue lines). For comparison Mn_{12} on Au(111) does not show these features (red line in the top left panel). (e) Simulated d^2I/dV^2 spectra using the 8-spin model (see text).

In Figure 3d typical experimental spectra are shown. The lowest excitation can be found in these examples at 1.4 meV (1.7 meV at 10 T) corresponding to a change of the m quantum number by one. The excitations observed at higher energy are due to an additional change of the total spin S of the molecule. For the latter several spin-configurations are possible and are the origin of the two energetically higher excitations observed at 4−9 meV and 11−16 meV, respectively. These excitations spread over relatively large range for different molecules presumably due to conformational changes that affect the fragile ligand field of Mn_{12} when adsorbed in different geometries on the surface.

At high tunneling rates in which the average time between two tunneling events is shorter than the lifetime of the excited state, one expects the pumping into states with higher energy.[22] The lifetime of the excited states can be estimated by the line width of the peaks in d^2I/dV^2 to be 2−4 ps. Thus, spin pumping would require tunneling currents of the order of 100 nA, which is too high for the fragile ligands of the molecule.

We note that the Coulomb blockade (CB) effect[23] cannot be responsible for the steplike structure in the dI/dV signal. CB steps would occur at an energy range of $e^2/2C$ with C as the capacity of the molecule in the tunnel junction. Estimating C for Mn_{12} on BN/Rh(111) results in CB energies of at least 100 meV, far beyond the energies of the spin-flip excitations discussed here (see Supporting Information). Furthermore, the observed excitations are not due to vibrational modes of the molecule which are expected at higher energies and have been found by IR and Raman spectroscopy on Mn_{12} at energies >25 meV.[24,25]

In summary, we demonstrated the controlled deposition of fragile Mn_{12} SMMs on metallic and thin-insulating surfaces and the feasibility of preserving the quantum magnetism of Mn_{12} on thin insulating layers such as BN. ES-IBD and local probe techniques such as STM are ideally suited for the preparation of complex molecular nanostructures and studying their properties. The added value provided by the combination of these two techniques is that the local electronic and magnetic properties derived from STM and STS investigations can be linked directly to a chemical structure, well characterized from the fully controlled, gentle deposition process that can be applied even to fragile molecules such as Mn_{12}. Our work provides access to atomic-scale studies of individual SMMs and their intriguing behavior, opening the pathway to experimentally address characteristics like tunneling of magnetization, lifetime of magnetization, or intermolecular coupling of magnetic moments.

Methods. Metal samples were prepared by subsequent Ar^+ sputtering and thermal annealing. The BN decoupling layer was prepared by exposing the clean Rh(111) surface to borazine gas while keeping it at 1070 K. $Mn_{12}O_{12}(CH_3COO)_{16}$ gas phase ions are generated by electrospray ionization at ambient pressure from a solution of $Mn_{12}O_{12}(CH_3COO)_{16}(H_2O)_4$ molecules in acetonitrile. ES-IBD proceeds through the transfer of the Mn_{12}^- ions into UHV through six differentially pumped vacuum chambers equipped with ion optics for collimation, mass selection, and focusing of the ion beam. Current monitoring, a retarding grid energy detector, and a TOF mass spectrometer allow to control the coverage, kinetic energy, and chemical composition.

To ensure intact deposition the ion beam is decelerated to a kinetic energy below 5 eV from an initial energy of 25−30 eV by applying an appropriate voltage to the sample. Afterwards, the sample is transferred in situ into either a commercial Omicron variable-temperature or a homemade He^4 Joule-Thompson cooled STM, the latter equipped with a superconducting 14 T magnet. We measure the differential conductance dI/dV by modulating the bias voltage (V_m = 0.5−1 mV, $f \approx 847$ Hz) and using lock-in detection. Bias voltage is applied to the sample.

■ ASSOCIATED CONTENT

Supporting Information

Additional information, figures, and references. This material is available free of charge via the Internet at http://pubs.acs.org.

■ AUTHOR INFORMATION

Corresponding Author

*E-mail: m.ternes@fkf.mpg.de.

dx.doi.org/10.1021/nl204141z | Nano Lett. 2012, 12, 518−521

Present Addresses

[‖]SPSMS, UMR-E CEA/UJF-Grenoble 1, INAC, Grenoble, F-38054, France.

[⊥]Instituto de Ciencia Molecular, Universitat de València, C/Catedrático José Beltrán 2, 46980 Paterna, Spain.

■ ACKNOWLEDGMENTS

We thank Fanny Schurz from the Max Planck Institute for Solid State Research for her work to synthesize the borazine. This work was financially supported by the Deutsche Forschungsgemeinschaft via the Collaborative Research Center SFB 767. The work of UCF group was supported by us-DOE grant DE-FG02-07ER46354.

■ REFERENCES

(1) Friedman, J. R.; Sarachik, M. P. *Ann. Rev. Condens. Matter. Phys.* **2010**, *1*, 109.
(2) Affronte, M. *J. Mater. Chem.* **2009**, *19*, 1731.
(3) Bogani, L.; Wernsdorfer, W. *Nat. Mater.* **2008**, *7*, 179.
(4) Affronte, M.; Troiani, F.; Ghirri, A.; Candini, A.; Evangelisti, M.; Corradini, V.; Carretta, S.; Santini, P.; Amoretti, G.; Tuna, A.; Timco, G.; Winpenny, R. E. P. *J. Phys. D: Appl. Phys.* **2007**, *40*, 2999.
(5) Sessoli, R.; Gatteschi, D.; Caneschi, A.; Novak, M. A. *Nature* **1993**, *365*, 141.
(6) Pineider, F.; Mannini, M.; Sessoli, R.; Caneschi, A.; Barreca, D.; Armelao, L.; Cornia, A.; Tondello, E.; Gatteschi, D. *Langmuir* **2007**, *23*, 11836.
(7) Voss, S.; Zander, O.; Fonin, M.; Rüdiger, U.; Burgert, M.; Groth, U. *Phys. Rev. B* **2008**, *78*, 155403.
(8) Mannini, M.; Sainctravit, P.; Sessoli, R.; Dit Moulin, C. C.; Pineider, F.; Arrio, M. A.; Cornia, A.; Gatteschi, D. *Chem.—Eur. J.* **2008**, *14*, 7530.
(9) Rogez, G.; Donnio, B.; Terazzi, E.; Gallani, J. L.; Kappler, J. P.; Bucher, J. P.; Drillon, M. *Adv. Mater.* **2009**, *21*, 4323.
(10) Saywell, A.; Magnano, G.; Satterley, C. J.; Perdigao, L. M. A.; Britton, A. J.; Taleb, N.; Del Carmen Gimenez-Lopez, M.; Champness, N. R.; O'Shea, J. N.; Beton, P. H. *Nat. Commun.* **2010**, *1*, 75.
(11) Ouyang, Z.; Takáts, Z.; Blake, T. A.; Gologan, B.; Guymon, A. J.; Wiseman, J. M.; Oliver, J. C.; Davisson, V. J.; Cooks, R. G. *Science* **2003**, *301*, 1351.
(12) Johnson, G. E.; Hu, Q.; Laskin, J. *Ann. Rev. Anal. Chem.* **2011**, *4*, 83.
(13) Rauschenbach, S.; Vogelgesang, R.; Malinowski, N.; Gerlach, J. W.; Benyoucef, M.; Costantini, G.; Deng, Z.; Thontasen, N.; Kern, K. *ACS Nano* **2009**, *3*, 2901.
(14) Berner, S.; Corso, M.; Widmer, R.; Groening, O.; Laskowski, R.; Blaha, P.; Schwarz, K.; Goriachko, A.; Over, H.; Gsell, S.; Schreck, M.; Sachdev, H.; Greber, T.; Osterwalder, J. *Angew. Chem.* **2007**, *46*, 5115.
(15) Bose, S.; García-García, A. M.; Ugeda, M. M.; Urbina, J. D.; Michaelis, C. H.; Brihuega, I.; Kern, K. *Nat. Mater.* **2010**, *9*, 550.
(16) Hirjibehedin, C. F.; Lutz, C. P.; Heinrich, A. J. *Science* **2006**, *312*, 1021.
(17) Hirjibehedin, C. F.; Lin, C. Y.; Otte, A. F.; Ternes, M.; Lutz, C. P.; Jones, B. A.; Heinrich, A. J. *Science* **2007**, *317*, 1199.
(18) Katsnelson, M. I.; Dobrovitski, V. V.; Harmon, B. N. *Phys. Rev. B* **1999**, *59*, 6919.
(19) Hennion, M.; Pardi, L.; Mirebeau, I.; Suard, E.; Sessoli, R.; Chaneschi, A. *Phys. Rev. B* **1997**, *56*, 8819.
(20) Mirebeau, I.; Hennion, M.; Casalta, H.; Andres, H.; Güdel, H. U.; Irodova, A. V.; Caneschi, A. *Phys. Rev. Lett.* **1999**, *83*, 628.
(21) Heersche, H. B.; De Groot, Z.; Folk, J. A.; Van der Zant, H. S. J.; Romeike, C.; Wegewijs, M. R.; Zobbi, L.; Barreca, D.; Tondello, E.; Cornia, A. *Phys. Rev. Lett.* **2006**, *96*, 206801.
(22) Loth, S.; Von Bergmann, K.; Ternes, M.; Otte, A. F.; Lutz, C. P.; Heinrich, A. J. *Nat. Phys.* **2010**, *6*, 340.
(23) Ingold, G. L.; Nazarov, Y. V. *NATO ASI Ser., B* **1992**, *294*, 21.
(24) Sushkov, A. B.; Musfeldt, J. L.; Wang, Y. J.; Achey, R. M.; Dalal, N. S. *Phys. Rev. B* **2002**, *66*, 144430.
(25) North, J. M.; Van de Burgt, L. J.; Dalal, N. S. *Solid State Commun.* **2002**, *123*, 75.

■ NOTE ADDED AFTER ASAP PUBLICATION

This article was published ASAP on December 27, 2011. Volodymyr Turkowski's name was misspelled. The corrected version was posted on December 30, 2011.